Available online at www.sciencedirect.com

SciVerse ScienceDirect

Energy Procedia 15 (2012) 229 – 239

Energy Procedia

International Conference on Materials for Advanced Technologies 2011, Symposium O

Fine-Tuning of Relative Fraction of Amorphous and Crystalline Phases in Hydrogenated Silicon Prepared by PE-CVD Method

A.M. Funde[a], V.S. Waman[b], M.M. Kamble[b], Pramod M.R.[b], S.P. Gore[b], G.R. Roze[b], V.G. Sathe[c], S.W. Gosavi[a] and S.R. Jadkar[a,*]

[a] *Department of Physics, University of Pune, Pune 411 007. India*
[b] *School of Energy Studies, University of Pune, Pune 411007. India*
[c] *UGC-DAE-CSR, University Campus, Indore 411 005. India*

Abstract

In the present study, nc-Si:H thin films have been deposited from rf-PE-CVD method. A set of depositions was achieved by varying deposition pressure from 234 mTorr to 1 Torr, while all other deposition parameters were kept constant. Structural, optical and electrical properties of the films were investigated in detail. Deposition pressure is found to be a crucial parameter in fine-tuning the material properties including relative fraction of amorphous and crystalline phases. Results indicate that film growth rate critically depends on plasma chemistry/gas phase chemistry governed by variation in deposition pressure. Deposition rate increased monotonically with increase in deposition pressure. Structural properties were studied by Raman spectroscopy and low angle XRD and the results shows that films are nanocrystalline over entire range of deposition pressure studied. Hydrogen content in the films was found < 11 at. % and decreases with increase in deposition pressure. Bandgap was found independent of deposition pressure while photoconductivity decreased by one order from 10^{-4} S/cm. Surface morphology of films was studied by AFM.

© 2011 Published by Elsevier Ltd. Selection and/or peer-review under responsibility of the organizing committee of International Conference on Materials for Advanced Technologies.

Keywords: Hydrogenated nanocrystalline silicon; PE-CVD; raman spectroscopy; atomic force microscopy; bandgap

1. Introduction

Hydrogenated silicon (Si:H) has been studied extensively as a basic material for thin film solar cells due to natural abundance of Si, environmental safety, potential high performance and being competent for

* Corresponding author. Tel.: +91 20 2569 5201; fax: +91 20 2569 5201
E-mail address: sandesh@physics.unipune.ac.in; adinathf@gmail.com

1876-6102 © 2011 Published by Elsevier Ltd. Selection and/or peer-review under responsibility of the organizing committee of International Conference on Materials for Advanced Technologies.
doi:10.1016/j.egypro.2012.02.027

low cost production. Extensive research has been carried out by many laboratories to improve the conversion efficiency of Si:H material based solar cells. The nc-Si:H is a material from this family that has been favoured than its amorphous counterparts due to its interesting properties such as high conductivity, high charge carrier mobility and high doping efficiency [1]. Furthermore, the nc-Si:H has better stability against the light-induced degradation compare to a-Si:H [2]. Another important advantage that nc-Si:H has got is the choices available as synthesis methods. The rf-PE-CVD is one such option and has been a preferred deposition method for nc-Si:H material. The PE-CVD has been proven for the industrial applicability among several other direct and indirect methods of depositing nc-Si:H material. The parameters affecting the deposition conditions and hence the material quality in PE-CVD are broadly divided in two categories [3], hardware parameters and process parameters. Both sets of parameters have been extensively studied for their effect on the material properties. The hardware parameters influencing the material quality are the electrode geometry [4], inter-electrode distance [5], and operating frequency [6]. The process parameters which are easily adjustable for a given reactor are the power density, deposition pressure, substrate temperature, and input gas flows.

The process parameters play a crucial role in determining the film properties in PE-CVD. These parameters affect the film properties in different ways and in order to obtain desired film properties an optimum set of parameters need to be selected. It is well known that the deposition pressure (P_{dep}) is one of the crucial parameters in PE-CVD. A detailed knowledge of influence of P_{dep} on structural and optical properties of nc-Si:H films is important for both the understanding fundamental physics of growth process as well as the fabrication of novel devices. However, so far there exist only few reports in the literature about the influence of deposition pressure on fundamental properties of nc-Si:H films. For example, the results obtained by Amanatides *et al.* [7] in this regard have shown that both electron density and energy are affected by the change of total pressure. The effect of increase of total gas pressure during deposition above 1 Torr, was initially studied by Guo *et al.* [8]. It was further intensely investigated by several other research groups [9-11]. It has been shown that it is possible to deposit device grade nc-Si:H thin films at deposition rates as high as 15 Å/s [12], while recent results have demonstrated high efficiency devices with nc-Si:H layers deposited at the pressure of 10 Torr [13]. However, there is lot of room for the improvement of film properties particularly at low deposition pressure because the relation between P_{dep} and structure and properties of the resulting films has not been elucidated yet. It is with this motivation that we initiated the detailed study of preparing nc-Si:H thin films at low deposition pressure (< 1 Torr). In this paper, we present the detail investigation of structural and optical properties of nc-Si:H films deposited by PE-CVD as a function of P_{dep}. It has been observed that these properties are greatly affected by the deposition pressure.

2. Experimental details

2.1. Film preparation

Films have been deposited in a conventional PE-CVD system (ANELVA, Japan), the details of which have been described elsewhere [14]. Films were prepared by glow discharge decomposition of SiH_4 (MSG) and H_2 (UHP) mixture. The films were deposited simultaneously on corning # 7059 glass to study optical and electrical properties and c-Si wafers (5-10 Ω-cm, p-type) to study structural properties. The flow rates of SiH_4 and H_2 were kept constant at 0.5 sccm and 75 sccm respectively and the deposition pressure is varied between 234 mTorr and 1 Torr using a throttle valve at suction port of the process chamber. With the present set of experiment, we restrict the deposition pressure between 234 mTorr and 1 Torr. We were unable to deposit the films below 234 mTorr due to ultimate suction capacity of vacuum

pumps. Other deposition parameters are listed in Table 1. The glass substrates were initially cleaned with in Piranha solution (H_2SO_4:H_2O_2 in the proportion of 4:1) after ultrasonic bath for 5 minutes and followed by wash in distilled water. Then dry nitrogen was flush to wipe off the water on the glass. The c-Si substrates were treated with HF to etch out native oxide layer. The substrates were loaded and the deposition chamber was evacuated to a base pressure less than 1×10^{-6} mTorr. Substrates were heated to the desired temperature by suitably setting the thermocouple and the temperature controller. The deposition was carried out for desired amount of time and films were allowed to cool to about 100 ^{0}C in vacuum. Then films were taken out for characterisation.

Table 1. Deposition parameters employed for the preparation of nc-Si:H thin films

Substrate temperature (T_{sub})	250 °C
Inter-electrode separation ($d_{e\text{-}s}$)	20 mm
Silane flow rate (F_{SiH4})	0.5 sccm
Hydrogen flow rate (F_{H2})	75 sccm
RF power	200 Watt
Deposition pressure (P_{dep})	234 mTorr to 1 Torr
Time of deposition (t)	40 min

2.2. Film characterisation

Dark conductivity (σ_{dark}) and photoconductivity (σ_{photo}) were measured with coplanar Al electrodes. The FTIR spectra of the films were recorded by using FTIR spectrophotometer (Shimadzu, Japan) and bonded hydrogen content in the films were estimated from integrated intensity of the 630 cm^{-1} for Si-H rocking/wagging absorption band using the method given by the Brodsky *et al.* [15]. The bandgap was estimated using the procedure followed by Tauc [16]. Raman spectra were recorded with micro-Raman spectroscopy (Jobin Yvon Horibra LABRAM-HR) in 400-700 cm^{-1} range. The spectrometer has backscattering geometry for detection of Raman spectrum with the resolution of 1 cm^{-1}. The excitation source was 632.8 nm line of He-Ne laser. The Raman spectra were de-convoluted in the range 420-560 cm^{-1} using Levenberg-Marquardt method [17] into their integrated crystalline, I_c (~520 cm^{-1}), amorphous, I_a (~480 cm^{-1}), and intermediate, I_m (~510 cm^{-1}) peaks. The crystalline fraction (X_{Raman}) was then deduced for 'large' crystallites and 'small' crystallites using the relations, $X_{Raman(large)} = I_c / (I_a + I_m + I_c)$ and $X_{Raman(small)} = I_m / (I_a + I_m + I_c)$ based as proposed by Sancho-Parramon *et al.*[18]. The crystallite size was calculated using the relation, $d_{Raman} = 2\pi(B/\Delta\omega)^{1/2}$, where $\Delta\omega$ is the peak shift compared to the c-Si and B = 2.0 cm^{-1}nm^2 [19]. Low angle x-ray diffraction spectra were obtained by x-ray diffractometer (Bruker D8 Advance, Germany) using Cu K_α line (λ = 1.54 Å). The spectra were taken at a grazing angle of 1^0. Average crystallite size was estimated using the classical Scherrer's formula, $d_{x\text{-}ray} = 0.9\lambda/B\cos\theta_B$ [20]. Thickness of films was determined by Talystep profilometer (Taylor-Hobson Rank). The particle size and surface topography of films were studied by AFM (JEOL, JSPM-5200, Japan).

3. Results and discussion

3.1. Variation in deposition rate

Films were deposited for a desired time period and the deposition rate is calculated from thickness measurement. The deposition rate (r_d) as a function of deposition pressure (P_{dep}) is plotted in Fig 1. As seen from the figure, r_d increases monotonically from ~1.8 Å/s to ~3.5 Å/s when P_{dep} increases from 234 mTorr to 1 Torr. The deposition of a film involves two simultaneous processes, first the deposition of the film-forming radicals and second being the etching of deposited material. Deposition rate is thus governed by the dominating nature between these two processes.

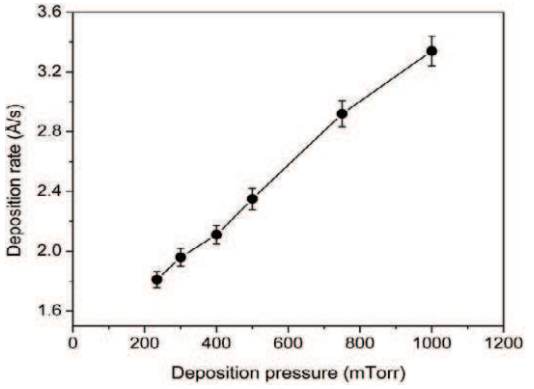

Fig. 1. Deposition rate as a function of deposition pressure. The vertical bars show the standard mean error.

Increase in deposition rate with increase in deposition pressure can be attributed to following factors:

- With increase in P_{dep}, the density of SiH_4 molecules in the process chamber increases. This results in an increase in number of film forming radicals due to increased ionisation of SiH_4. So, deposition rate increases with increase in deposition pressure.
- Increase in P_{dep} leads to increase in secondary gas phase reactions and reaction products. Atomic H is depleted through secondary gas phase reactions. Consequently, etching of growing material due to atomic H decreases. Thus, deposition rate increases with increase in deposition pressure.
- Increase in P_{dep} also increases the dwell time of radicals in plasma. It increases the probability that generated radicals will reach to the substrate and contribute to the film growth. Thus, overall deposition rate increases with increase in deposition pressure.

3.2. Raman spectroscopy analysis

The Raman spectra obtained for films deposited different deposition pressures (P_{dep}) are shown in Fig. 2(a). The spectra have been normalised for maximum intensity and plotted with constant vertical shift for better clarity. Each spectrum shown in Fig. 2(a) was de-convoluted into three Gaussian peaks with a quadratic base line method. Figure 2(b) represents a typical de-convoluted Raman spectra for the nc-Si:H film prepared at P_{dep} = 234 mTorr. As seen from Fig. 2(a), all films have a broad peak centred ~ 520 cm^{-1} which is a characteristic of nc-Si:H. In addition, shift of this peak towards lower wavenumber has been observed with increase in deposition pressure. These results suggest decrease in crystalline fraction in the film with increase in deposition pressure. The crystalline volume fraction decrease from ~75 % to 68 % when deposition pressure increases from 234 mTorr to 1 Torr (see Table 2).

The crystallite size was calculated for two phases, 'small' crystallites (peak between 500 and 510 cm^{-1}) and 'large' crystallites (peak ~520 cm^{-1}) [18]. Finally, the overall crystallite size is estimated by taking the ratio of large and small crystallites which is shown in the last column of Table 2. The overall crystallite size decreases from ~12.8 nm to ~ 3.1 nm as deposition pressure increased from 234 mTorr to 1 Torr. Increase in deposition pressure plays an important role in determining material properties by controlling the plasma chemistry. At lower P_{dep}, radicals reaching the surface are mainly SiH_3 and H [21]. So, the growth surface is well covered with SiH_3 and H radicals. They diffuse in the growing surface result in the growth of nano-crystallisation. But with increase in P_{dep}, density of SiH_x radicals reaching the growth

surface gets increased and this limits the growth of the nano-crystallites [15, 21]. This is amplified in the form of reduction of overall crystallite size in the films and increase in amorphous content.

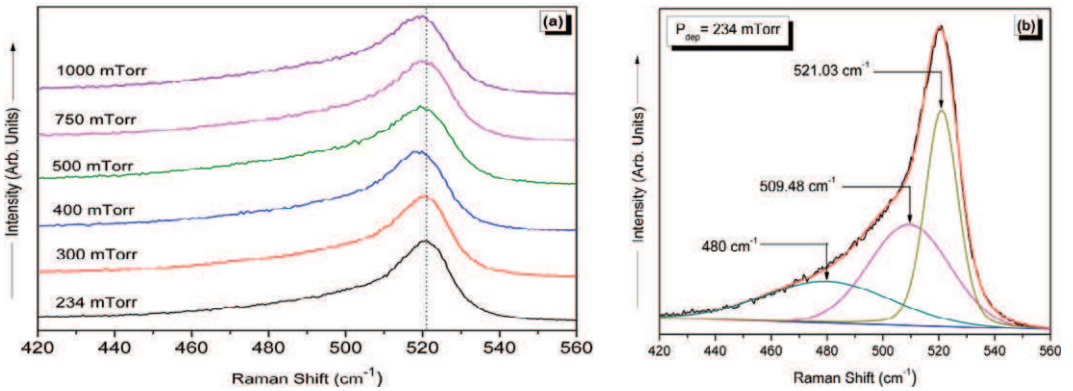

Fig. 2. (a) Raman spectra of the films deposited at different deposition pressure; (b) A typical de-convoluted Raman spectrum for the film deposited at P_{dep} = 234 mTorr

Table 2. Detail analysis of the Raman spectra of the film deposited at different deposition pressures (P_{dep})

Deposition Pressure (mTorr)	Crystalline Volume Fraction (X_{Raman}) %	Size of Small Crystallites (nm)	Size of Large Crystallites (nm)	Overall Crystallite Size d_{Raman} (nm)
234	75.2	2.6	33.4	12.8
300	74.0	2.4	15.3	6.4
400	70.2	2.5	11.7	4.7
500	67.3	2.4	12.5	5.2
750	69.8	2.5	10.2	4.1
1000	68.3	2.6	08.0	3.1

3.3. Low-angle x-ray diffraction analysis

Figure 3 shows the x-ray diffraction pattern of films deposited at various deposition pressures (P_{dep}). As seen from the figure the films deposited for entire range of P_{dep}, were nanocrystalline. Furthermore, it is seen from the pattern that the films have preferred crystallographic orientation along the (111) plane, whereas (220) and (311) were also observed with lesser intensity.

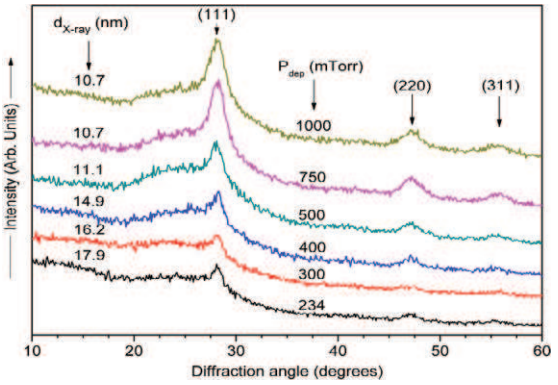

Fig. 3. X-ray diffraction patterns of the films deposited by varying deposition pressures

Qualitatively, it is clearly seen that the FWHM of the pattern increases with increasing P_{dep}. This is also supported by quantitative data of the average crystallite size estimated by the classical Scherrer's formula. The values of average crystallite size for films deposited at different P_{dep} as estimated by the classical Scherrer's formula are also shown in Fig. 3. The average crystallite size of the nc-Si:H grains goes on declining monotonically from ~18 nm to ~10 nm when P_{dep} increases from 234 mTorr to 1 Torr. These results are consistent with the crystallite size estimated from the Raman spectroscopic measurements as depicted in the Table 2. The main common observation in the crystallite size estimation from these two analysis techniques can be noted as the decrease in the average crystallite size with increasing deposition pressure. The difference observed in crystallite size estimated from these two analysis techniques is due to the difference in the working principles of the techniques. Thus, x-ray diffraction results supports the crystallite size results obtained from that of Raman Spectroscopy and confirms independently the preferred crystallographic orientation to be (111).

3.4. Atomic force microscopy (AFM) analysis

In pursuit of topographical aspects of deposited films, we carried out AFM investigations. Figure 4 depicts surface topography investigated by AFM for the films deposited at P_{dep} = 300, 500 and 1000 mTorr. With increase in deposition pressure (P_{dep}), significant differences in structure can be seen.

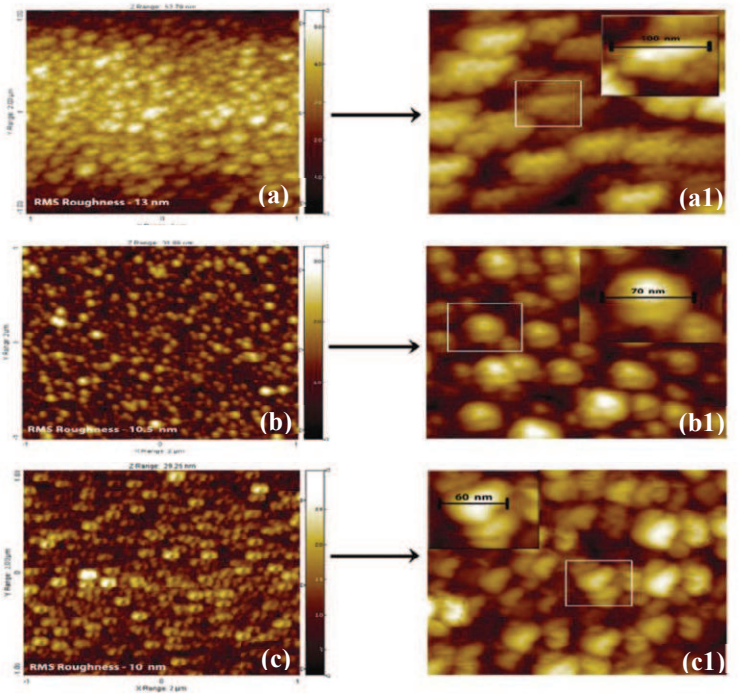

Fig. 4. AFM images of films deposited at (a) 300 mTorr; (b) 500 mTorr; (c) 1000 mTorr scanned on 2 µm × 2 µm area. Images on right side of the arrow of each [(a1);(b1);(c1)] are scanned over 500 nm × 500 nm and single particle with average size is shown in inset.

As seen from the Fig. 4(a), the films deposited at P_{dep} = 300 mTorr, show a large number of spherical shape particle agglomerates are observed indicating nanocrystalline nature of the material. For this film the average particle size is ~100 nm and RMS surface roughness ~13 nm. With increase in deposition

pressure i.e. the films deposited at P_{dep} = 300 mTorr and 1 Torr, show well resolved, small and non-uniform grains indicating biphasic (amorphous + nanocrystalline) nature of the material. The average grain size and surface roughness for these films were ~70 and 60 nm and ~10 and 10.5 nm, respectively. These results suggest that with increasing deposition pressure the films prepared by PE-CVD become porous and defective. Difference between the average grain size determined by Raman, XRD and AFM techniques has been reported previously [22-23].

3.5. FTIR spectroscopic analysis

To reveal the hydrogen bonding configuration and to estimate the total hydrogen content in the films, FTIR spectroscopy is used. Figure 5(a) shows the FTIR spectra for some Si:H films deposited at various deposition pressure. The horizontal break between 1100 cm^{-1} to 1700 cm^{-1} is added for better clarity. As seen from the figure, the films deposited at P_{dep} = 234 mTorr have major absorption bands at ~ 630 cm^{-1} and ~ 2000 cm^{-1}, which correspond to the wagging vibrational modes of different bonding configurations and the stretching vibrational mode of mono-hydrogen (Si-H) bonded species respectively [24, 25].

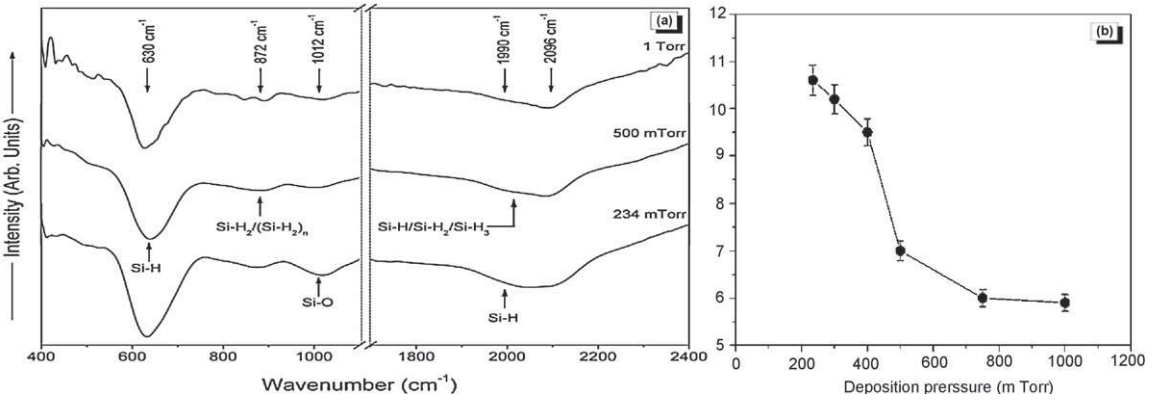

Fig. 5. (a) FTIR transmission spectra of some films, the respective deposition pressure values are labelled for each spectrum. Horizontal break between 1100 cm^{-1} to 1700 cm^{-1} is added for better clarity; (b) Calculated values of bonded hydrogen content as a function of deposition pressure. The vertical bars show the standard mean error in estimation of hydrogen content.

The spectrum also exhibits bending vibrational mode between 800-900 cm^{-1} associated with $Si-H_2$ and $(Si-H_2)_n$ complexes (isolated or coupled) [26] with lesser intensity. These results clearly indicate that at low deposition pressure the hydrogen is predominantly incorporated in the films in Si-H bonding configuration. In addition to these vibrational modes, an absorption peak at ~1014 cm^{-1} associated with the asymmetric Si-O-Si stretching vibration is also seen in the FTIR spectrum for the films deposited at lower deposition pressure. This is indicative of an oxidation effect caused by its porous-like microstructure, which is a typical feature for nc-Si:H thin films [27]. However, with increase in deposition pressure the absorption of 631 cm^{-1} band decreases. At the same time, the absorption of band at ~2000 cm^{-1} shift towards higher wave number and its intensity increases with increase in process pressure. Thus, the film deposited at P_{dep} = 1 Torr show similar bands, but with additional absorption peak at ~2100 cm^{-1}. According to the literature, the absorption peak ~ 2100 cm^{-1} corresponds to stretching vibrational modes of $Si-H_2$ and $(Si-H_2)_n$ species [28, 29]. Furthermore, to confirm the various stretching modes of hydrides present in the films, the FTIR spectra were de-convoluted in the range 1800 cm^{-1} to

2200 cm^{-1} [30]. These results clearly indicate that with increase in deposition pressure hydrogen bonding in the films shifts from Si-H bonded species to $Si-H_2$ and $(Si-H_2)_n$ complexes.

It was found that the hydrogen content in Si:H materials calculated from different methods is quite different. However, it has been reported that the integrated intensity of the peak at ~630 cm^{-1} is the best measure of hydrogen content and other bands are less reliable [31]. Whatever may be the nature of the hydrogen bonding configuration; Si-H, $Si-H_2$, $(SiH_2)_n$, SiH_3 etc., all types of the vibrational modes will contribute to the 630 cm^{-1} absorption band [32]. Thus, the hydrogen content has been estimated using integrated intensity of the peak at 630 cm^{-1}. Figure 5(b) shows the variation of hydrogen content (C_H) as a function of deposition pressure (P_{dep}). As seen from the figure, C_H in the film decreases from ~10.6 at. % to ~5.9 at. % as P_{dep} increases from 234 mTorr to 1 Torr. We attribute the decrease in C_H with increasing the P_{dep} to decrease in crystallinity in the film with increase in deposition pressure. In nc-Si:H normally, the Si nanocrystals are embedded in amorphous tissue or otherwise the nanocrystalline grains are surrounded by amorphous part and most hydrogen is incorporated at grain boundaries or grain boundary tissue. Appearance of the absorption peak at ~2100 cm^{-1} together with the wagging mode absorption in the range 800-900 cm^{-1} in the FTIR spectra and enhancement in their intensity with increase in deposition pressure supports this.

3.6. Variation in bandgap

The influence of deposition pressure (P_{dep}) on the band gap (E_g) is shown in Fig. 6. It can be seen from the figure that the bandgap is almost independent on the deposition pressure employed for the synthesis nc-Si:H films by PE-CVD method.

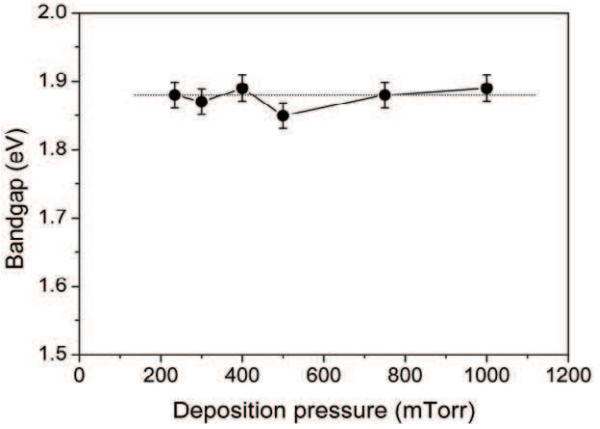

Fig. 6. Variation of bandgap as a function of deposition pressure for nc-Si:H films deposited by PE-CVD method. The vertical bars show the standard mean error in estimation of bandgap.

It is accepted that the bandgap depends on the hydrogen content and it increases with the increase in hydrogen content in the films [33]. However, in the present investigations, the bandgap is found almost constant over the entire range of deposition pressure studied indicating that the amount of bounded hydrogen only cannot account for the bandgap in nc-Si:H films. In addition, there exist several ambiguities about the bandgap of nc-Si:H films because the material contains both, amorphous and crystalline phases. The typical value of the bandgap of hydrogenated amorphous silicon (a-Si:H) is

between 1.6 and 1.8 eV depending on the process parameters. Accordingly, in the case of a mixed phase of crystalline and amorphous, i.e. nanocrystalline phase, the bandgap should lie between amorphous and crystalline silicon [34]. However, in the present case, we have observed high bandgap values (~1.9 eV) over the entire range of deposition pressure employed. We think that such high bandgap values are may be due to the presence of micro-voids in the films. These micro-voids reduce the effective density of the material and increase average Si-Si distance [35]. This lowers the absorption in the film and shifts the transmission curve towards higher photon energy. This produces higher optical bandgap, which is estimated by extrapolation of absorption curve on the energy axis.

3.7. Electrical conductivity measurement

Figure 7 shows the dependence of dark conductivity (σ_{Dark}) and photoconductivity (σ_{Photo}) of nc-Si:H films deposited at various deposition pressures (P_{dep}). As seen from the figure, both the σ_{Dark} and the σ_{Photo} decrease from ~ 10^{-4} S/cm to ~ 10^{-5} S/cm when P_{dep} increases from 234 mTorr to 1 Torr. As a result, the films didn't show any photosensitivity gain. This is expected because films were nanocrystalline over the entire range of deposition pressure studied as revealed by Raman spectroscopic (Fig. 2) and low angle XRD (Fig. 3) studies because the nc-Si:H films prepared by different methods show negligible photosensitivity depending upon the crystallite size and its volume fraction [36].

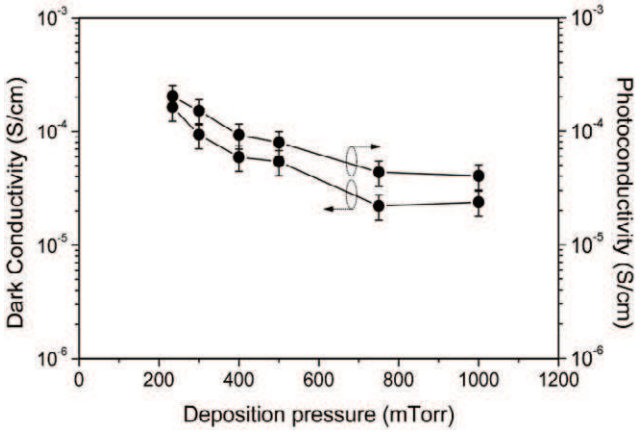

Fig. 7. Variation of dark conductivity and photo conductivity as a function of deposition pressure. The vertical bars show the standard mean error.

4. Conclusions

Hydrogenated nanocrystalline silicon (nc-Si:H) thin films were deposited using PE-CVD system by varying the deposition pressure from 234 mTorr to 1 Torr. The structural, optical and electrical properties of the deposited films were investigated in detail. Deposition rate increases monotonically from 1.8 Å/s to 3.3 Å/s with increase in deposition pressure. Raman spectroscopy and low-angle x-ray diffraction results show that the films are nanocrystalline over entire range of deposition pressure studied. Both crystallite size and crystalline volume fraction have shown decreasing trend. The surface topography studies using atomic force microscopy indicates that average particle size as well as RMS surface roughness decreases with increase in deposition pressure. The FTIR spectroscopy results indicate that with increase in deposition pressure hydrogen bonding in the films shifts from $Si-H_2$ and $(Si-H_2)_n$ to Si-H bonded species.

Bonded hydrogen content in the films was found below 11 at. % and decreases to ~6 at. % with increase in deposition pressure. However, the bandgap was found independent of deposition pressure. From the present study it has been concluded that the deposition pressure is a key process parameter to induce the crystallinity in the Si:H films by PE-CVD. The ease of depositing films with tuneable crystallite size and its volume fraction is useful for fabrication of tandem solar cells. However, further detailed experiments are required to study the effect of other process parameters to optimise the nc-Si:H films before starting n- and p-type doping for solar cells applications.

Acknowledgements

Financial assistance to AMF from Department of Science and Technology (DST), Government of India from International Travel Support Scheme to participate in ICMAT2011 is gratefully acknowledged. The authors SRJ, AMF, VSW, PMR and MMK are thankful to DST and Ministry of New and Renewable Energy (MNRE), Govt. of India and also to the Centre for Nanomaterials and Quantum Systems (CNQS), University of Pune for financial support.

References

[1] Lee C, Sazonov A, Nathan A. High-mobility nanocrystalline silicon thin-film transistors fabricated by plasma-enhanced chemical vapor deposition. *Appl. Phys. Lett.* 2005; **86**: 222106.

[2] Mahan AH. Hot wire chemical vapor deposition of Si containing materials for solar cells. *Sol. Energy Mater. Sol. Cells* 2003; **78**: 299.

[3] Bugnon G, Feltrin A, Meillaud F, Bailat J, Ballif C. Influence of pressure and silane depletion on microcrystalline silicon material quality and solar cell performance. *J. Appl. Phys.* 2009; **105**: 064507.

[4] Niikura C, Kondo M, Matsuda A. Preparation of microcrystalline silicon films at ultra high-rate of 10 nm/s using high-density plasma. *J. Non-Cryst. Solids* 2004; **42**: 338-40.

[5] Amanatides E, Mataras D, Rapakoulias DE. Combined effect of electrode gap and radio frequency on power deposition and film growth kinetics in SiH_4/H_2 discharges. *J. Vac. Sci. Technol. A* 2002; **20**: 68.

[6] Shah AV, Meier J, Vallat-Sauvain E, Wyrsch N, Kroll U, Droz C *et al*.. Material and solar cell research in microcrystalline silicon. *Sol. Energy Mater. Sol. Cells* 2003; **78**: 469.

[7] Amanatides E, Hammad A, Katsia E, Mataras D. High pressure regime of plasma enhanced deposition of microcrystalline silicon. *J. Appl. Phys.* 2005; **97**: 073303.

[8] Guo L, Kondo M, Fukawa M, Saitoh K, Matsuda A. High rate deposition of microcrystalline silicon using conventional plasma-enhanced chemical vapor deposition. *Jpn. J. Appl. Phys.* 1998; **37/2**: L1116.

[9] Rath JK, Franken RHJ, Gordijn A, Schropp REI, Goedhee WJ. Growth mechanism of microcrystalline silicon at high pressure conditions. *J. Non-Cryst. Solids* 2004; **338**: 56.

[10] Tanda M, Kondo M, Matsuda, A. A novel approach for the growth of μc-Si at a high rate over 3 nm/s. *Thin Solid Films* 2003; **427**: 33.

[11] Smets AHM, Matsui T, Kondo M. High-rate deposition of microcrystalline silicon *p-i-n* solar cells in the high pressure depletion regime. *J. Appl. Phys.* 2008; **104**: 034508.

[12] Kondo M, Fukawa M, Guo L, Matsuda A. High rate growth of microcrystalline silicon at low temperatures. *J. Non-Cryst. Solids* 2000; **84**: 266-9.

[13] Rech B, Roschek T, Repmann T, Muller J, Schmitz R, Appenzeller W. Microcrystalline silicon for large area thin film solar cells. *Thin Solid Films* 2003; **427**: 157.

[14] Funde AM, Bakr NA, Kamble DK, Hawaldar RR, Amalnerkar DP, Jadkar SR. Influence of hydrogen dilution on structural, electrical and optical properties of hydrogenated nanocrystalline silicon (nc-Si:H) thin films prepared by plasma enhanced chemical vapour deposition (PE-CVD). *Sol. Energy Mater. Sol. Cells* 2008; **92**: 1217.

[15] Brodsky MH, Cardona M, Cuomo JJ. Infrared and Raman spectra of the silicon-hydrogen bonds in amorphous silicon prepared by glow discharge and sputtering. *Phys. Rev. B* 1977; **16**: 3556.

[16] Tauc J. Optical properties of solids. In: Abeles F, editor. *Optical properties of solids*, North-Holland, Amsterdam; 1972, p. 277.

[17] Marquardt DW. An algorithm for least-squares estimation of nonlinear parameters. *J. Soc. Ind. Appl. Math* 1963; **11 (2)**: 431.
[18] Sancho-Parramon J, Gracin D, Modreanu M, Gajovic A. Optical spectroscopy study of nc-Si-based p–i–n solar cells. *Sol. Energy Mater. Sol. Cells* 2009; **93**: 1768-72.
[19] He Y, Yin C, Cheng G, Wang L, Lie X, Hu GY. The structure and properties of nanosize crystalline silicon films. *J. Appl. Phys.* 1994; **75**: 797.
[20] Cullity BD, Stock SR. *Elements of X-ray diffraction*. 3rd ed., Prentice Hall; 2001.
[21] Katsia E, Amanatides E, Mataras Soto DA, Voyiatzis GA. Total SiH_4/H_2 pressure effect on microcrystalline silicon thin films growth and structure. *Sol. Energy Mater. Sol. Cells* 2005; **87**: 157.
[22] Bardet E, Bouree JE, Cuniot M, Diximier J, Elkaim P, Middya AR *et al*.. The grain size in microcrystalline silicon: correlation between atomic force microscopy, UV reflectometry, ellipsometry, and X-ray diffractometry. *J. Non-Cryst. Solids* 1996; **198**: 867.
[23] Gutierrez JJ, Inglefield CE, An CP, DeLong MC, Taylor P, Morrison S *et al*.. Structural characterization of SiF_4, SiH_4, and H_2 hot-wire grown microcrystalline silicon thin films with large grains. *Mat. Res. Soc. Symp. Proc.* 2001; **664**:A 3.4.
[24] Wei W, Xub G, Wang J, Wang T. Raman spectra of intrinsic and doped hydrogenated nanocrystalline silicon films. *Vacuum* 2007; **81**: 656.
[25] Lucovsky G. Vibrational spectroscopy of hydrogenated amorphous silicon alloys. *Solar Cells* 1980; **2**: 431.
[26] Montero I, Galan L, Najmi O, Albella JM. Disorder-induced vibration-mode coupling in SiO_2 films observed under normal-incidence infrared radiation. *Phys. Rev. B* 1994; **50**: 4881.
[27] Halindintwali S, Knoesen D, Swanepoel R, Julies BA, Arendse C, Muller T *et al*.. Improved stability of intrinsic nano-crystalline Si thin films deposited by hot-wire chemical vapour deposition technique. *Thin Solid Films* 2007; **515**: 8040.
[28] Molenbroek EC. Deposition of hydrogenated amorphous silicon with hot-wire technique. [PhD thesis]. University of Colorado; USA: 1995.
[29] Das C, Ray S. Onset of microcrystallinity in silicon thin films. *Thin Solid Films* 2002; **403**: 81.
[30] Smets AHM, Matsui T, Kondo M. Infrared analysis of the bulk silicon-hydrogen bonds as an optimization tool for high-rate deposition of microcrystalline silicon solar cells. *Appl. Phys. Lett.* 2008: **92**:033506.
[31] Shanks HR, Fang CJ, Cardona M, Demond FJ, Kalbitzer S. Infrared spectrum and structure of hydrogenated amorphous silicon. *phys. status solidi b* 1980; **100**: 43-56.
[32] Lau WS. *Infrared Characterization of Microelectronics*; World Scientific: Singapore 1999.
[33] Tauc J, Grigorovici R, Vancu A. Optical properties and electronic structure of amorphous germanium. *phys. status solidi b* 1966; **15**: 627.
[34] Rotaru C, Nastase S, Tomozeiu N. Amorphous phase influence on the optical bandgap of polysilicon. *phys. status solidi a* 1999; **171**: 365.
[35] Crandall RS, Liu X, Iwaniczko E. Recent developments in hot wire amorphous silicon. *J. Non-Cryst. Solids* 1998; **227-230**: 23.
[36] Saitoh T, Shimada T, Migitaka M, Preparation and properties of microcrystalline silicon films using photochemical vapor deposition. *J. Non-Cryst. Solids* 1983; **59-60**: 715.